Al-Qadisiyah Journal of Pure Science

Volume 29 | Number 2 Article 6

12-20-2024

Effect of RF power on optical, structural and gas sensor Characteristics of ZnO thin films prepared by RF plasma.

Mustafa H. hashim
Physics Department,College of Education/University Al-Qadisiya,Iraq country

Abdulhussain A. khadayeir
Physics Department,College of Education/University Al-Qadisiya,Iraq country,
abdulhussain.khadyair@qu.edu.iq

Recommended Citation

hashim, Mustafa H. and khadayeir, Abdulhussain A. (2024) "Effect of RF power on optical, structural and gas sensor Characteristics of ZnO thin films prepared by RF plasma.," *Al-Qadisiyah Journal of Pure Science*: Vol. 29 : No. 2 , Article 6.
Available at: https://doi.org/10.29350/2411-3514.1283

ARTICLE

Effect of RF Power on Optical, Structural and Gas Sensor Characteristics of ZnO Thin Films Prepared by RF Plasma

Mustafa H. Hashim, Abdulhussain A. Khadayeir*

Physics Department, College of Education, University Al-Qadisiya, Iraq

Abstract

This paper investigates, the effect of RF power on the structural, optical properties of ZnO thin films. It was prepared by RF magnetic sputtering at 400 °C on a glass substrate. And working pressure (5×10^{-2} Torr), and different energy values (50, 70 W). The effect of different radiofrequency powers. X-ray diffraction (XRD) and (Uv-Vis) methods were used to explore the structural and optical characteristics of thin films. The growth rate and much more increased when the RF power was increased. The results on the crystal structure demonstrated that polycrystalline patterns are common in nature for all produced ZnO thin films, the hexagonal phase as well as the (002) plane's favored direction. The grain size of the films was determined between (14−20 nm), indicating that all of these films had a nanocrystalline structure. Data on the optical properties of the produced films The ZnO film was ideal for solar cell applications because it had excellent transmittance values in the visible region (95 %), The energy gap was within the range of (3.30−3.34 eV) for pure zinc oxide films prepared with different values of power, and we note that there is a slight increase in the energy gap when increasing the power. Gas sensors were tested at various mixing ratios (NO2 97 %, air 3 %) and operational temperatures (25, 100, 200, and 300 °C) and using a bias voltage (6V). A temperature of about 300 °C was found to be the ideal working temperature for the sample. Greatest sensitivity (88 %) with a quick response time (17 s) and the fastest recoveries (63 s), which take place at a temperature of 300 °C. The result we came to was that the impact of power on the surface topography and Crystal structure induced the creation of large-surface-area nanocrystals, which is highly advantageous, and raises the sensor's sensitivity.

Keywords: RF power, ZnO thinfilms, NO_2 gas, Structural & optical characteristics

1. Introduction

ZnO is well recognized for use in a variety of applications, including gas sensors, transistor transparent conductors, and solar cells. Light detectors, laser diodes, and light emitting diodes (LEDs) are further developing uses. These applications have the following are attributed to the intriguing material characteristics of a large and direct band gap (3.37 eV) and strong binding energy [1,2]. It is appealing for possible usage in electronics, optoelectronics, and laser technology due to has high mechanical and thermal stability at room temperature [3]. ZnO thin films were created using a variety of deposition processes, such as the sol-gel techniques, spray pyrolysis, pulsed laser deposition, and magnetron sputtering [4−7]. The sputtering procedure is the method for creating ZnO thin film that is the most promising of them, Ideal sputtering conditions include mechanical assembly, good surface flatness, high deposition rate, formation of dense layers, transparency, and its possibility for low-temperature processing [8,9]. For chemical dangerous gas sensing, research has been focused on nano crystalline n-type semiconductor metal oxide gas sensors, such as (NO_2, SO_2, H2S, H_2, CH_4, CO_2, ethanol (C_2H_5OH)) and volatile organic compounds [10−15]. Nanostructured gas detectors metal

Received 22 April 2022; accepted 28 June 2022.
Available online 18 April 2025

* Corresponding author.
E-mail addresses: mhaydar815@gmail.com (M.H. Hashim), abdulhussain.khadyair@qu.edu.iq (A.A. Khadayeir).

https://doi.org/10.29350/2411-3514.1283

oxides with a variety of morphologies, including nanorods [16], nanotubes [17], nanosheets [18], nanowires [19], nanospheres [20] and synthesizeable nano-thin sheets using a variety of methods. These metal oxide-based nanostructure gas sensors with a variety of topologies allowed for the detection of these various gases [10,14,15]. Due to the harmful effects of polluting gases on human health, it is now crucial for industrial operations to monitor air pollution, air quality, and safety [10,12]. Gases that cause pollution that are released from combustion equipment and transportation, principally contain NOx pollutants (NO and NO_2), whatever of the fuel quality, As a result, gas sensors are increasingly common and perform crucial roles in a variety of industrial applications, including the detection of methane, hydrocarbons, ammonia, and hydrogen gas in fuel cells, mining, oil refineries, and fertilizer sectors [15,17]. Different types of metal oxides-based gas sensors, which use semiconductors such (SnO_2, Fe_2O3, CuO, TiO_2, ZnO and Ca_2O_3) which were employed for the detection of dangerous chemical gases and polluting gases [12,15,21]. Some factors, including surface morphology, nanostructure type and dimension, which has a significant surface to volume ratio and nano size in contrast to bulk materials, can govern the gas sensor's responsiveness [11,12,15]. ZnO gas sensors work by measuring changes in electrical resistivity at the sensor surface brought on by the reducing and oxidizing of gases. Additionally, ZnO gas sensors are widely employed in a variety of applications due to its affordability, non-toxicity, ease of fabrication, high stability, high responsiveness, and superior selectivity [12,15,22]. This paper study ZnO thin film in using a RF sputtering technique, and the effect of RF power on structural, optical characteristics was taken into consideration to reach the maximum level of transparency. Using a UV-Vis spectrophotometer and x-ray diffraction (XRD), the characteristics of the ZnO films were investigated. The goal of this research was to establish the ideal RF sputtering power.

2. Experimental details

2.1. Materials & methods

By using an RF magnetron sputtering approach with a 5-inch diameter The RF magnetron spraying system consists of three main parts: RF power source, vacuum pump, and vacuum chamber. Manufactured by Zhengzhou CY Scientific Instrument Co., Ltd., China. Fig. 1 shows the RF system 99.99 % pure ZnO target, the ZnO film was deposited to glass substrates at 400 °C. In an ultrasonic bath for 10 min, the substrate was first washed with distilled water, ethanol, and acetone. Following this, before sedimentation, the substrates were dried and cleaned with distilled water. Grease and organic particles were taken out of the substrate throughout the cleaning procedure. The deposition time was (120 min) and the working pressure was 5×10^{-2} Torr, and the substrate temperature was 400 °C. Coating was done using RF spray power (50 and 70 W). Equation was used to measure the thickness of the films (t) using the weighing method: $t = \frac{\Delta m}{\rho A}$ where, Δm: shows the mass difference between the slide before and after the deposition, A: area of the film, ρ: mass density. The

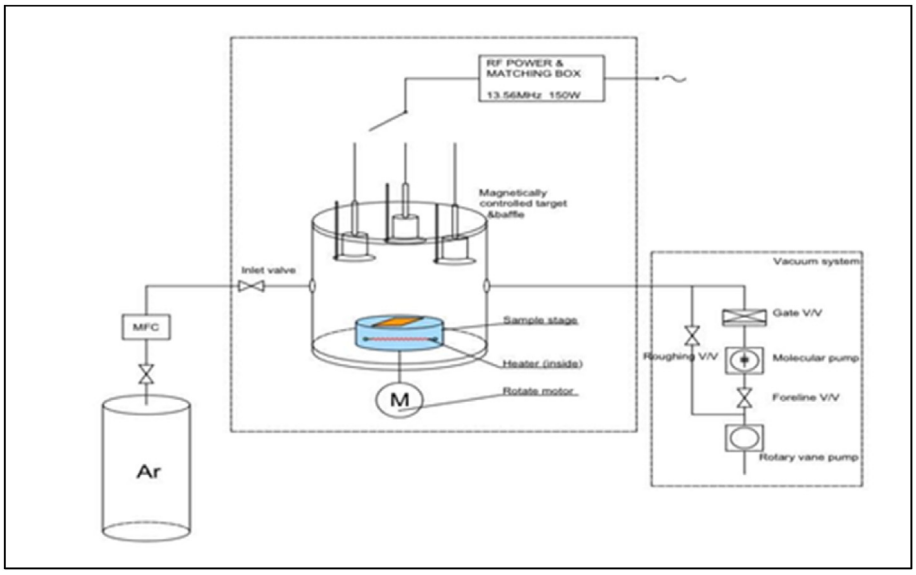

Fig. 1. RF system for deposition of ZnO films of different power.

thickness of the films prepared (200 nm). By using an X-ray diffraction technique using a Cu-Kα radiation source (XRD-6000) Shimadzu, Japan; = (1.54060 A^0), the system was operated at 40 kV to examine the crystal structure of the zinc oxide films. The angle range of the scan was 2°, and the scanning speed was 5° per minute. For the checking of optical characteristics, a Mega 2100 UV-VIS Double-beam spectrophotometer, with a wavelength range of (300–900 nm) was employed.

2.2. Manufacturing of gas sensors

On a glass substrate, ZnO thin-film gas sensors were created by RF method. Using a thermal evaporation system, the electrodes were fabricated with a thickness of (300 nm) by thermal evaporation in a vacuum. Through the evaporation of 99.9 % pure aluminum wire in a spiral tungsten boat under (10^{-7}) mbar of pressure Fig. 2a, b Al electrodes and gas sensor measuring equipment. The gas-air mixture was managed by the flow meter.

3. Results & discussions

Fig. 3(a) show that the RF power grows from (50–70 W), the spray power has an effect on the growth rate with the increase in the growth rate. This phenomenon develops due to the presence of more argon ions in the plasma at greater RF energies, causing more atoms to be dispersed when the ions accelerate and hit the target [1]. In addition, more atoms are sprayed because bombardment ions have higher kinetic energy at higher RF strengths due to momentum transfer [23]. The atom that is dispersed gains more energy at In comparison to lower RF energies, the increased RF energy caused more ZnO particles to reach the substrate. Increase the levels of the power and aids in the development of the film [24].

Fig. 4 shows the produced ZnO thin films' XRD spectra as the RF power changes from (50 W–70 W). The peak with the highest intensity was found at $2\theta = 34.38°, 34.46^{o}$ which corresponds to the (002) plane and having a hexagonal structure. Orientation along the c-axis. The ZnO films' tops fit the standard ICDD card (JCPDS #36–1451). Allowed for the effective deposition of ZnO thin films with various RF powers onto the glass substrate. The working pressure has been maintained at (5×10^{-2} Torr). Equation was used to get the (d-spacing) for pure ZnO thin films [25]:

$$\frac{1}{d_{hkl}^2} = \frac{4}{3}\frac{(h^2+hk+k^2)}{a^2} + \frac{l^2}{c^2} \quad (1)$$

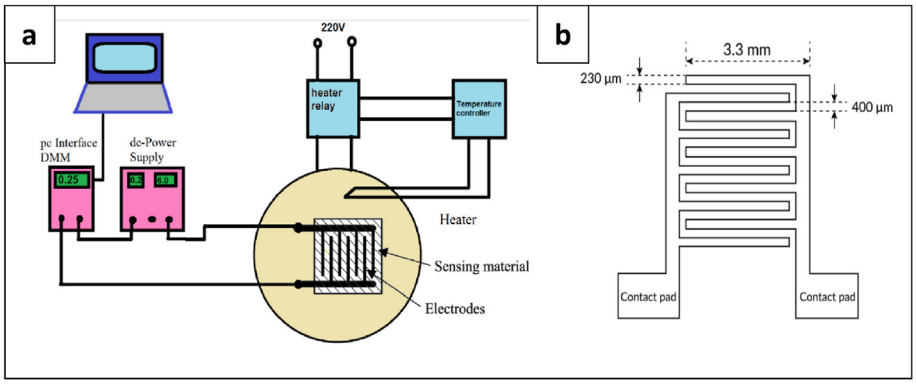

Fig. 2. (a) System for measuring gas sensors, (b) Electrodes to measure gas sensitivity.

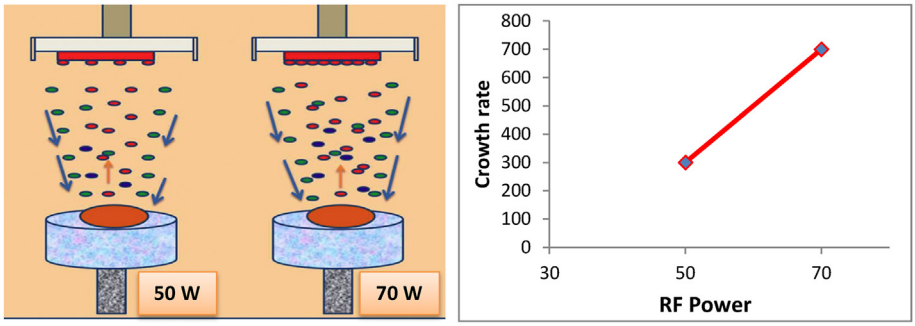

*Fig. 3. **(a)** Diagram illustrating the influence of RF power, **(b)** Relationship between growth rate and sputtering strength of ZnO films.*

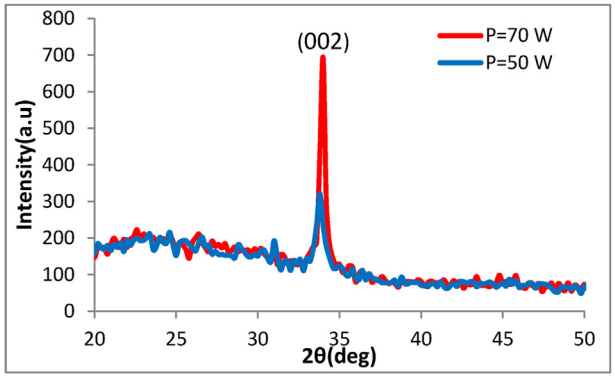

Fig. 4. Shows the XRD pattern of ZnO thin films deposited at different powers (50, 70 W).

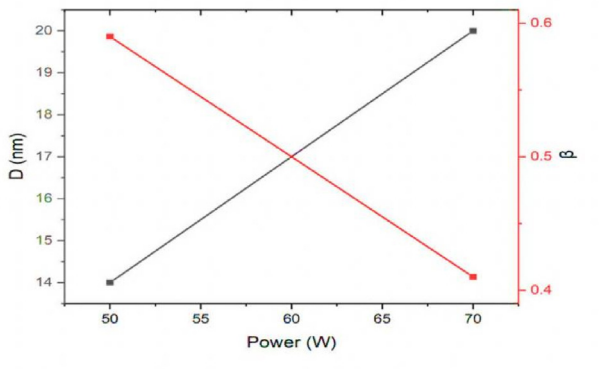

Fig. 5. Grain size and the variation of (FWHM) of ZnO at different RF power (50, 70 W).

Values were in good agreement with the (JCPDS) card data and are provided in Table 1. Where, d: distance between crystal planes.

The Scherrer formula may be used to get the average crystallite size (D) as shown below [26]:

$$D = \frac{0.9\lambda}{\beta \, Cos \, \theta} \tag{2}$$

D: the crystalline size, λ: the (XRD) wavelength (0.154 nm), θ: the Bragg angle and β: FWHM (rad). With the increase of the RF energy, the size of the crystals also increases and (FWHM) decreases because the relationship between them is inverse according to the Scherrer formula. The average grain size values confirm the thin films' nanostructure characteristic as deposited as they range inside the nano scale, as shown in Table 1. The crystal size increases from 14 to 20 when the RF power is increased from (50–70 W), as shown in Fig. 5.

4. Optical characteristics

Fig. 6(a) shows the transmittance spectra for the samples deposited at various sputtering powers (50,70 W) as a function of wavelength in the spectrum visible. A UV-Vis spectrophotometer was used to test the optical transmittance between the wavelengths of (300–900 nm). The thickness of the samples, as measured by the weighing method (200 nm). All of the thin films had transmittance levels of around 95 %, (visible range) with greater transmittance being attained in the blue range than the red range. The films' fundamental absorption edges were moved in the direction of shorter wavelengths (blue shift). The most vital factor in the use of thin films as a transparent electrode or as a buffer layer in solar cells is their great transparency. The predicted energy band gap of ZnO may be calculated using the Tauc relation [27]:

$$(\alpha hv)^{1/2} = A(hv - E_g) \tag{3}$$

Were, A: constant for transition, hv: Photon energy (eV), α: absorption coefficient.

Fig. 6(b) is show a diagram of the film's energy (hv) versus absorption coefficient $(hv)^2$, at different values of power (50,70W). The value of the energy gap (eV) was computed to meet the requirement that $(hv)^{1/2} = 0$. For as-deposited ZnO films, E_g values range from 3.30 eV to 3.34 eV.

Table 1. ZnO thin films' X-ray diffraction data analysis at pressure 5×10^{-2} Torr.

RF Power(W)	d_{xrd} (A°)	d_{sta} (A°)	2θ (deg)	hkl	β (deg)	D (nm)
50	2.63	2.60	34.38	002	0.56	14
70	2.64	2.60	34.46	002	0.41	20

5. Measuring the sensing

To determine the sensing characteristics and sensitivity of ZnO films sensors for NO2 gas, sensing measurements are examined at various NO_2:air mixing ratios (3 % air, 97 % NO_2) and With bias voltage (6V) and at different operating temperature ranging from (25–300 °C). Where the allergic response of the prepared films with a power of 70 W and 50 W at the mentioned temperatures was a response to the pure film. And the resistance values decrease when the temperature is increased because it is a reversible process and this characteristic is characteristic of semiconductor materials [28]. The process of oxygen molecule adsorption and desorption on the ZnO surface is primarily used to characterize the mechanism of gas detection in ZnO sensors. When ZnO nanostructures are exposed to air, oxygen molecules adsorb on the grain surface and generate O_2^-, O^{-2}, and O^-, which creates a depletion layer close to the grain's surface. The

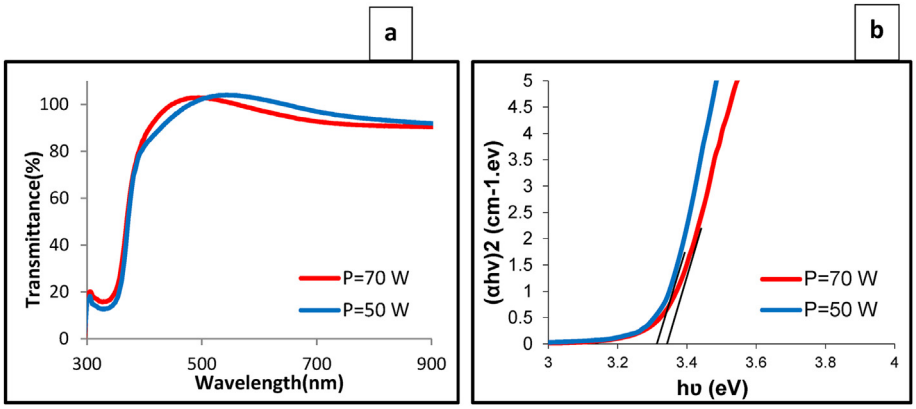

Fig. 6. (a) Transmittance for a Zno thin films as a function of wavelength, (b) plots $(\alpha hV)^2$ and (hv) for ZnO thin films at RF power at (50–70 W).

electrons are captured during this adsorption, increasing the resistance of the active layer in the process. The following relationships might explain the chemical reaction [29,30]:

$$O_2(g) \rightarrow O_2(ads) \quad (4)$$

$$O_2 + e^- \rightarrow O_2^-(ads) \quad (5)$$

$$O_2^-(ads) + e^- \rightarrow 2O^-(ads) \quad (6)$$

When an oxidizing gas, such as NO_2, is present near the sensor, the molecules of the gas capture electrons from the ZnO conduction band, and interact with the oxygen types that have been adsorbed 0n the surface of the material. This increases the electron depletion layer and increases the junction potential barriers, which raises the sensor's resistance and produces a sensing response. The following relationships provided the chemical reactions [29,31]:

$$NO_2^-(ads) + e^- \rightarrow NO_2^-(ads) \quad (7)$$

$$NO_2^-(ads) + O_2^-(ads) + e^- \rightarrow 2O^-(ads) + NO_2^-(ads) \quad (8)$$

$$NO_2^-(ads) + O^-(ads) + 2e^- \rightarrow 2O_2^- + NO(gas) \quad (9)$$

$$NO_2^-(ads) + h^+ \rightarrow NO_2(gas) \quad (10)$$

When the sensor is re-released into the air, NO_2^- reacts with the holes and the electrons are returns to the conduction band permitting the release of NO_2 into the air and lowering resistance [30]. ZnO gas sensor sensitivity From the NO_2: air mixing ratios (3 % air, 97 % NO_2), were measured using the equation [32]:

$$S = \frac{R_{gas} - R_{air}}{R_{air}} \times 100\% \quad (11)$$

Where, R_{gas}: Electrical resistance in the presence of gas.

R_{air}: Electrical resistance in the presence of air.

Fig. 7 shows the sensitivity of the pure zinc oxide film prepared at different values of power (50, 70 W) to NO_2 gas.

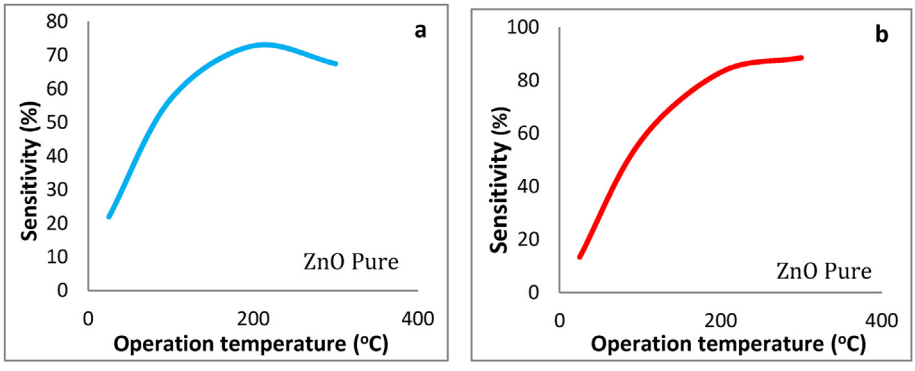

Fig. 7. The sensitivity of zinc oxide to no2 gas a function of temperature at a power of (a) 50 W, (b) 70 W.

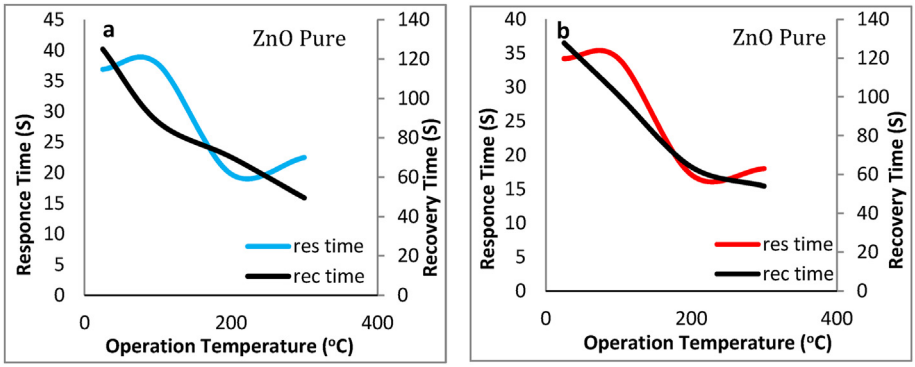

Fig. 8. Rresponse times, recovery times of 97 % NO_2 a function of the operating temperature of ZnO films prepared at different values of power (a) 50 W, (b) 70 W.

The sensitivity was calculated using equation (11) for pure ZnO thin films at different values of power (50, 70 W), after measuring the resistance of the samples in the presence of air (R_{off}) and the presence of gas (R_{on}). The highest value reached at the temperature 300 °C and its value was (88.5 %) at the power 70 W, while the highest value was at the temperature of 200 °C and its value was (72.7 %) at the power 50 W. Obtaining the highest sensitivity response by NO_2 gas molecules as shown in Fig. 8 for membranes with different energy values (50, 70 W). The response time (which represents the interaction time between the gas and the thin film during the sensing process), back to the initial state, was measured. Response time is one of the important factors in determining the efficiency of the sensor, the faster the response, the more efficient the sensor at the appropriate operating temperature. The response time was in the range (17–19 s) and the recovery time was in the range (70-63 s) for films prepared at power (70, 50 W). The highest response obtained was (17 s) for the prepared (70 W) ZnO film.

6. Conclusions

In the present research, RF-magnetron spray was used to create ZnO thin films at various power RF, a substrate temperature of 400 °C, and a constant working pressure. Analysis was done on the structural and optical characteristics of the ZnO thin films. The deposited ZnO thin films show a high orientation along the c-axis, according to the XRD pattern, the greatest peak occurring at a diffraction angle of (34.38°, 34.46°) which corresponds to the (002) plane of the ZnO (hexagonal) phase. All films are very transparent (95 %) in the visible domain, according to transmission measurement. This paper illustrates the potential of ZnO thin films for solar cells and window layers in the future. It may be concluded from the study's findings on the features of gas sensors that the gas ZnO film sensors had excellent sensitivity and high selectivity for NO_2 gas. According to the ZnO sensor's parameters, the response times were between (17–19 s), the recovery (63–70 s). The highest sensitivity was 88 % for ZnO film at 300 °C, when the film prepared at 70 W. These values are considered optimal, making the ZnO sensor a useful gas sensor appropriate for gas detector applications. Hazardous and flammable.

Funding

Self-funding.

References

[1] Lu, Yang-Ming, Hwang Weng-Sing, Liu WY, Yang JS. Effect of RF power on optical and electrical properties of ZnO thin film by magnetron sputtering. Mater Chem Phys 2001;72(2): 269–72.
[2] Zhang Yangyang, Ram Manoj K, Stefanakos Elias K, Yogi Goswami D. Synthesis, characterization, and applications of ZnO nanowires. J Nanomater 2012;2012:20.
[3] Kołodziejczak-Radzimska Agnieszka, Jesionowski Teofil. Zinc oxide—from synthesis to application: a review. Materials 2014;7(4):2833–81.
[4] Ayouchi R, Martin F, Leinen D, Ramos-Barrado JR. Growth of pure ZnO thin films prepared by chemical spray pyrolysis on silicon. J Cryst Growth 2003;247(3):497–504.
[5] Nagayasamy Nagarani, Gandhimathination Saroja, Veerasamy Vasu. The effect of ZnO thin film and its structural and optical properties prepared by sol-gel spin coating method. Open J Met 2013;2013.
[6] Musa Mohamed Zahidi, Mamat Mohamad Hafiz, Rusop Mohamad. Electrical characteristic of UV sensor using nanostructured Al doped ZnO thin film. Adv Mater Res 2013; 667:384–7. Trans Tech Publications.
[7] Ilican S, Caglar Y, Caglar M. Preparation and characterization of ZnO thin films deposited by sol-gel spin coating method. J Optoelectron Adv Mater 2008;10(10):2578–83.
[8] Lin Su-Shia, Huang Jow-Lay. Effect of thickness on the structural and optical properties of ZnO films by rf magnetron sputtering. Surf Coating Technol 2004;185(2):222–7.
[9] Kim Hyoun Woo, Nam Ho Kim. Structural studies of room-temperature RF magnetron sputtered ZnO films under

different RF powered conditions. Mater Sci Eng, B 2003; 103(3):297−302.
[10] Wanga J, Fana S, Xiab Y, Yanga C, Komarnenic S. Room-temperature gas sensors based on ZnO nanorod/Au hybrids: visible light-modulated dual selectivity to NO2 and NH3. J Hazard Mater 2020;381:120919.
[11] Chaoa J, Chena Y, Xingb S, Zhanga D, Shena W. Facile fabrication of ZnO/C nanoporous fibers and ZnO hollow spheres for high performance gas sensor. Sensor Actuator B Chem 2019;298:126927.
[12] Hsueh T, Peng C, Chen W. A transparent ZnO nanowire MEMS gas sensor prepared by an ITO microheater. Sensor Actuator B Chem 2020;304:127319.
[13] Choudhury SP, Feng Z, Gao C, Ma X, Zhan J, Jia F. BN quantum dots decorated ZnO nanoplates sensor for enhanced detection of BTEX gases. J Alloys Compd 2020;815:152376.
[14] Cao P, Yang Z, Navale ST, Han S, Liu X, Liu W, Lu Y, Stadler FJ, Zhu D. Ethanol sensing behavior of Pd-nanoparticles decorated ZnO-nanorod based chemiresistive gas sensors. Sensor Actuator B Chem 2019;298:126850.
[15] Bhati VS, Hojamberdiev M, Kumar M. Enhanced sensing performance of ZnO nanostructures-based gas sensors: a review. Energy Rep 2020;6:46−62.
[16] Fang F, Futter J, Markwitz A, Kennedy J. UV and humidity sensing properties of ZnO nanorods prepared by the arc discharge method. Nanotechnology 2009;20:245502.
[17] Kaviyarasu K, Mola GT, Oseni SO, Kanimozhi K, Maria Magdalane C, Kennedy J, Maaza M. ZnO doped single wall carbon nanotube as an active medium for gas sensor and solar absorber. J Mater Sci Mater Electron 2019;30(1):147−58.
[18] Jiaqiang Xu, Xue Z, Qin N, Cheng Z, Xiang Q. The crystal facet-dependent gas sensing properties of ZnO nanosheets: experimental and computational study. Sensor Actuator B Chem 2017;242:144−57.
[19] Guo J, Zhang J, Zhu M, Dianxing Ju, Hongyan Xu, Cao B. High-performance gas sensor based on ZnO nanowires functionalized by Au nanoparticles. Sensor Actuator B Chem 2014;199:339−45.
[20] Rathnakumar SS, Noluthando K, Kulandaiswamya AJ, Rayappan JBB, Kasinathan K, Kennedy J, Maaza M. Stalling behavior of chloride ions: a non-enzymatic electrochemical detection of α-endosulfan using CuO interface. Sensor Actuator B Chem 2019;293:100−6.
[21] Wales DJ, Grand J, Ting VP, Burke RD, Edler KJ, Bowen CR, Mintova S, Burrows AD. Burrows, gas sensing using porous materials for automotive applications. Chem Soc Rev 2015; 44:4290−321.
[22] Rai P, Kim Y-S, Song H-M, Song M-K, Yu Y-T. The role of gold catalyst on the sensing behavior of ZnO nanorods for CO and NO2 gases. Sens Actuators B 2012;165:133−42 (2012).
[23] Hwang Deuk-Kyu, Kyu-Hyun Bang, Jeong Min-Chang, Myoung Jae-Min. Effects of RF power variation on properties of ZnO thin films and electrical properties of p−n homojunction. J Cryst Growth 2003;254(3):449−55.
[24] Yu Xuhu, Ma Jin, Ji Feng, Wang Yuheng, Zhang Xijian, Cheng Chuanfu, Ma Honglei. Effects of sputtering power on the properties of ZnO: Ga films deposited by rf magnetronsputtering at low temperature. J Cryst Growth 2005; 274(3):474−9.
[25] Cullity BD. Elements of X-ray diffraction. Third printing. University of Notre Dame Indiana; 1967.
[26] Azaroff LV. Elements of X-ray crystallography. New York: McGraw-Hill; 1968.
[27] Junfei Shi, Dong Chengyuan, Wenjun Dai, Jie Wu, Chen Yuting, Runze Zhan. The influence of RF power on the electrical properties of sputtered amorphous In—Ga—Zn—O thin films and devices. J Semiconduct 2013;34(8):084003.
[28] Korotcenkov G. Handbook of gas sensor materials. New York: Springer LLC; 2013.
[29] Ganapathi KS, Kaur M, Shaheera M, Pathak A, Gadkari SC, Debnath AK. Highly sensitive NO2 sensor based on ZnO nanostructured thin film prepared by SILAR technique. Sensor Actuator B Chem 2021;335:129678.
[30] Choi MS, Kim MY, Mirzaei A, Kim H-S, Kim S, Baek S-H, Chun DW, Jin C, Lee KH. Selective, sensitive, and stable NO2 gas sensor based on porous ZnO nanosheets. Appl Surf Sci 2021;568:150910.
[31] Al-Hardan N, Abdullah MJ, Abdul Aziz A. The gas response enhancement from ZnO film for H2 gas detection. Appl Surf Sci 2011;255:7794−7.
[32] Nguyen H, Quy CT, Hoa ND, Lam NT, Van Duy N, Van Quang V, Van Hieu N. Controllable growth of ZnO nanowires grown on discrete islands of Au catalyst for realization of planartype micro gas sensors. Sens Actuators B 2014;193: 888−94.